

Supplementary Materials

**Microwave-pulse assisted synthesis of tunable ternary-doped 2D molybdenum carbide for efficient hydrogen evolution**

**Miao Fan<sup>#</sup>, Jiayue Guo<sup>#</sup>, Guangyu Fang<sup>#</sup>, Haoran Tian, Yongfei You, Zhenhui Huang, Jingru Huang, Huiyu Jiang, Weilin Xu, Jun Wan<sup>\*</sup>**

State Key Laboratory of New Textile Materials and Advanced Processing Technologies, Hubei Key Laboratory of Biomass Fibers and Eco-Dyeing & Finishing, Wuhan Textile University, Wuhan 430200, Hubei, China.

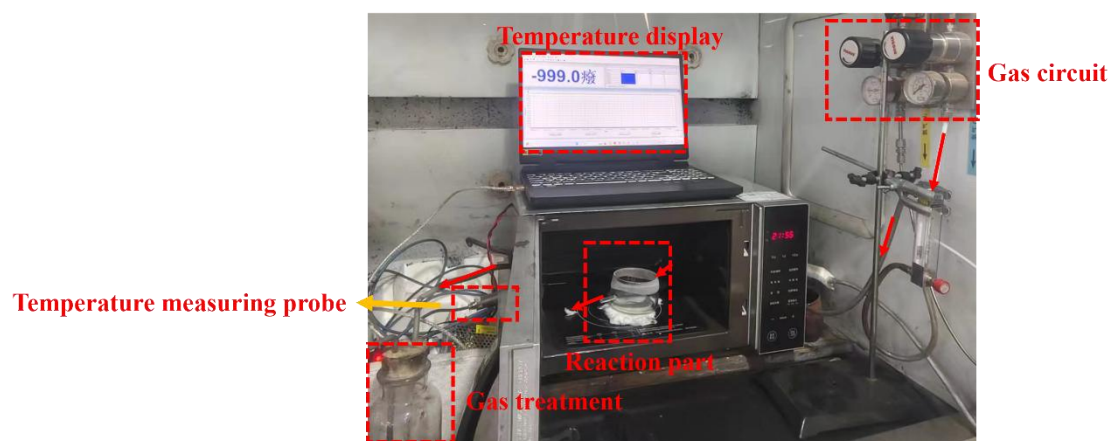
<sup>#</sup>Authors contributed equally.

**\*Correspondence to:** Prof. Jun Wan, State Key Laboratory of New Textile Materials and Advanced Processing Technologies, Hubei Key Laboratory of Biomass Fibers and Eco-Dyeing & Finishing, Wuhan Textile University, 1 Sunny Avenue, Wuhan 430200, Hubei, China. E-mail: wanj@wtu.edu.cn

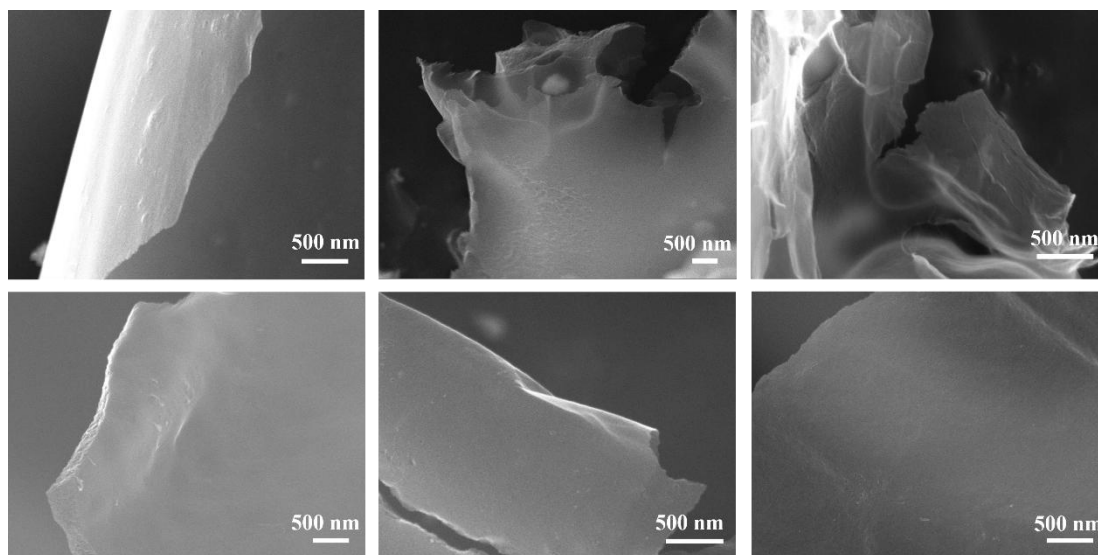
1. Supplementary Figures 1-17
2. Supplementary Tables 1-3
3. References



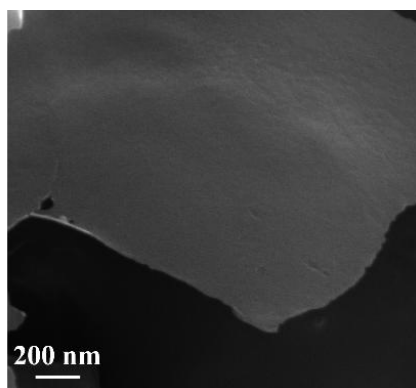
## 1. Supplementary Figures 1-17



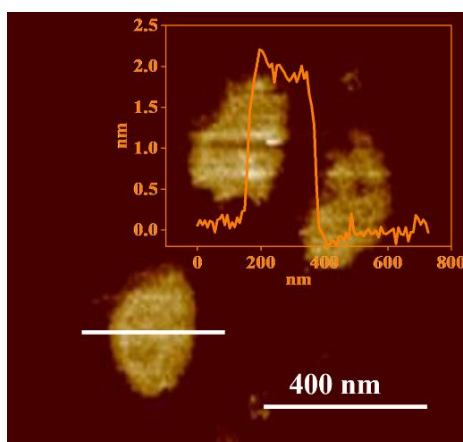
**Supplementary Figure 1.** Detailed optical picture of microwave pulse reaction equipment.



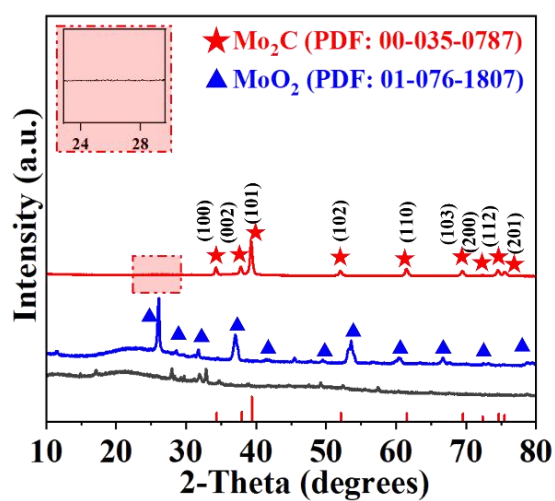
**Supplementary Figure 2.** (A-F) SEM images of 2D P-Mo<sub>2</sub>C, 2D N-Mo<sub>2</sub>C, 2D S-Mo<sub>2</sub>C, 2D P,N-Mo<sub>2</sub>C, 2D P,S-Mo<sub>2</sub>C, 2D N,S-Mo<sub>2</sub>C, respectively.



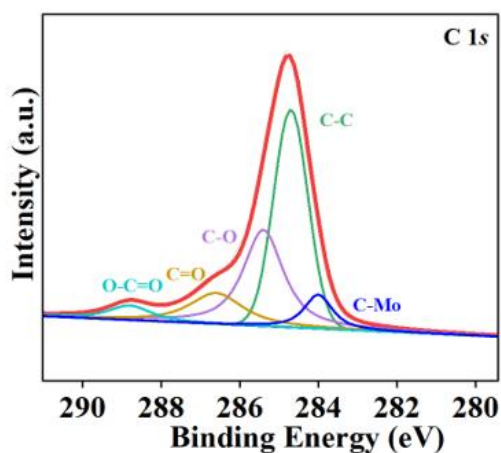
Supplementary Figure 3. SEM images of 2D Mo<sub>2</sub>C.



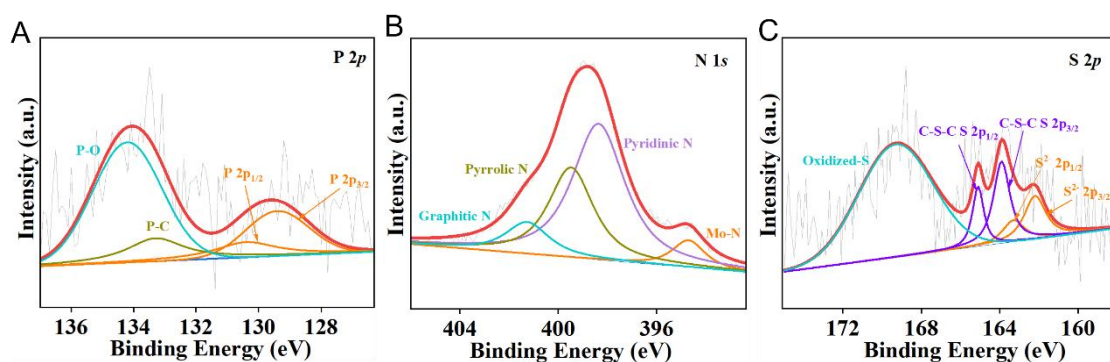
Supplementary Figure 4. AFM images of 2D P,N,S-Mo<sub>2</sub>C.



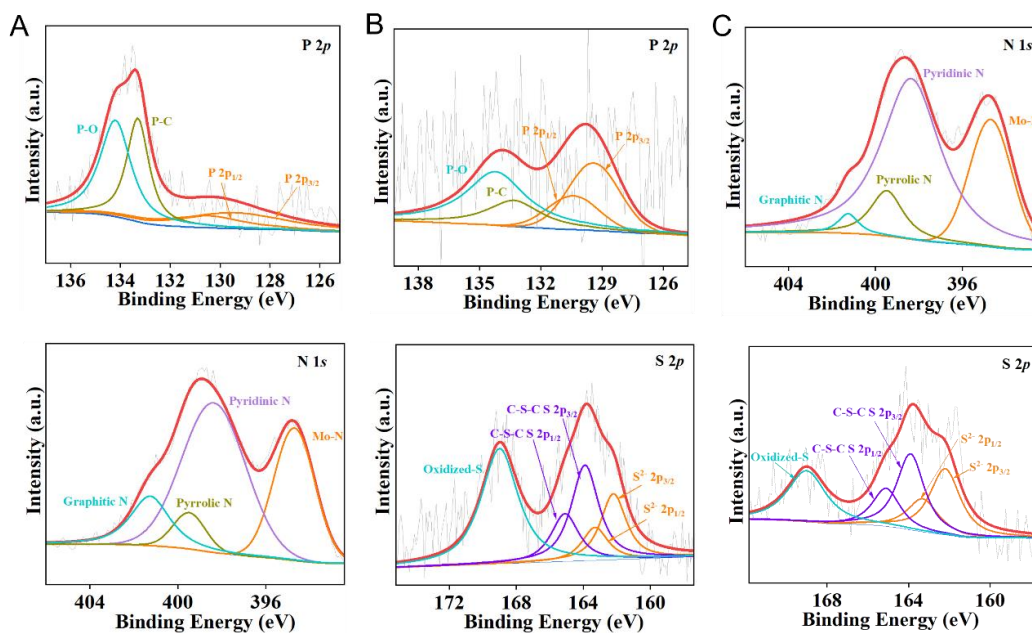
Supplementary Figure 5. XRD patterns of T<sub>1</sub>, T<sub>2</sub> and T<sub>3</sub>, respectively.



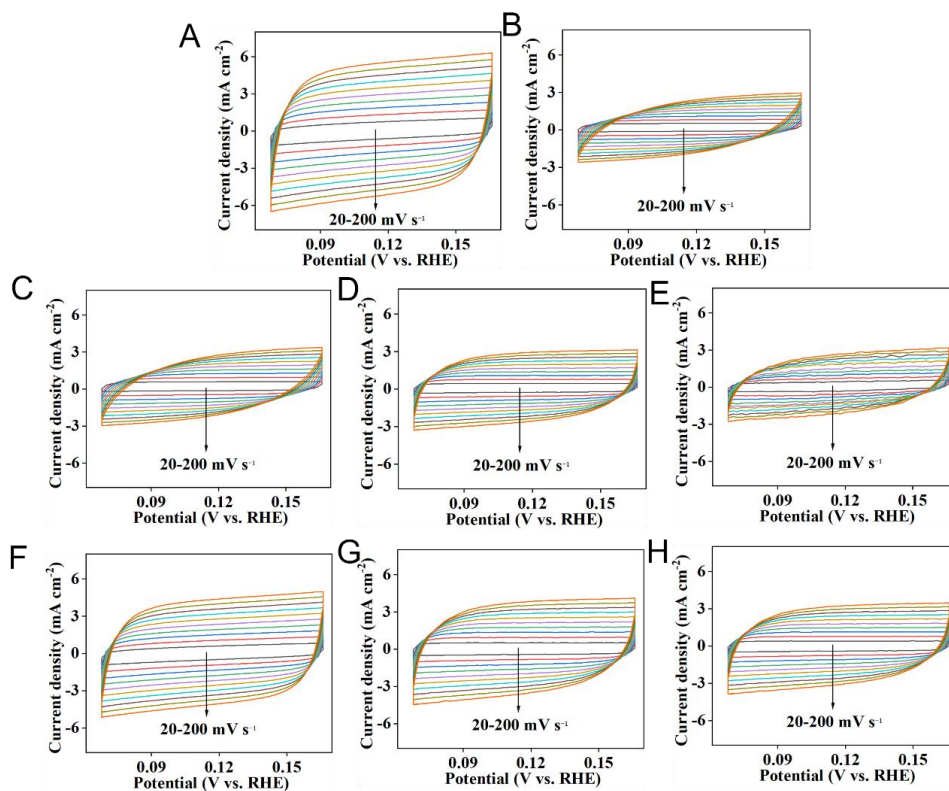
**Supplementary Figure 6.** C 1s spectrum of 2D P,N,S-Mo<sub>2</sub>C.



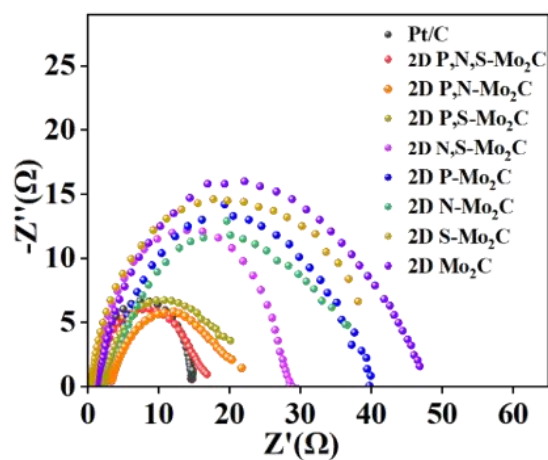
**Supplementary Figure 7.** (A) High-resolution XPS spectra of P 2*p* for 2D P-Mo<sub>2</sub>C. (B) High-resolution XPS spectra of N 1*s* for 2D N-Mo<sub>2</sub>C. (C) High-resolution XPS spectra of S 2*p* for 2D S-Mo<sub>2</sub>C.



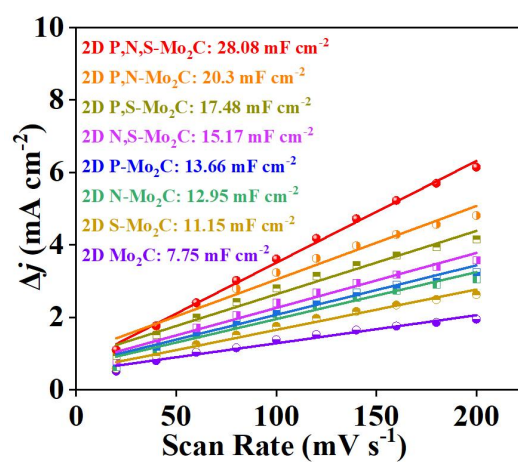
**Supplementary Figure 8.** (A) High-resolution XPS spectra of N 1s and P 2p for 2D P,N-Mo<sub>2</sub>C. (B) High-resolution XPS spectra of P 2p and S 2p for 2D P,S-Mo<sub>2</sub>C. (C) High-resolution XPS spectra of N 1s and S 2p for 2D N,S-Mo<sub>2</sub>C.



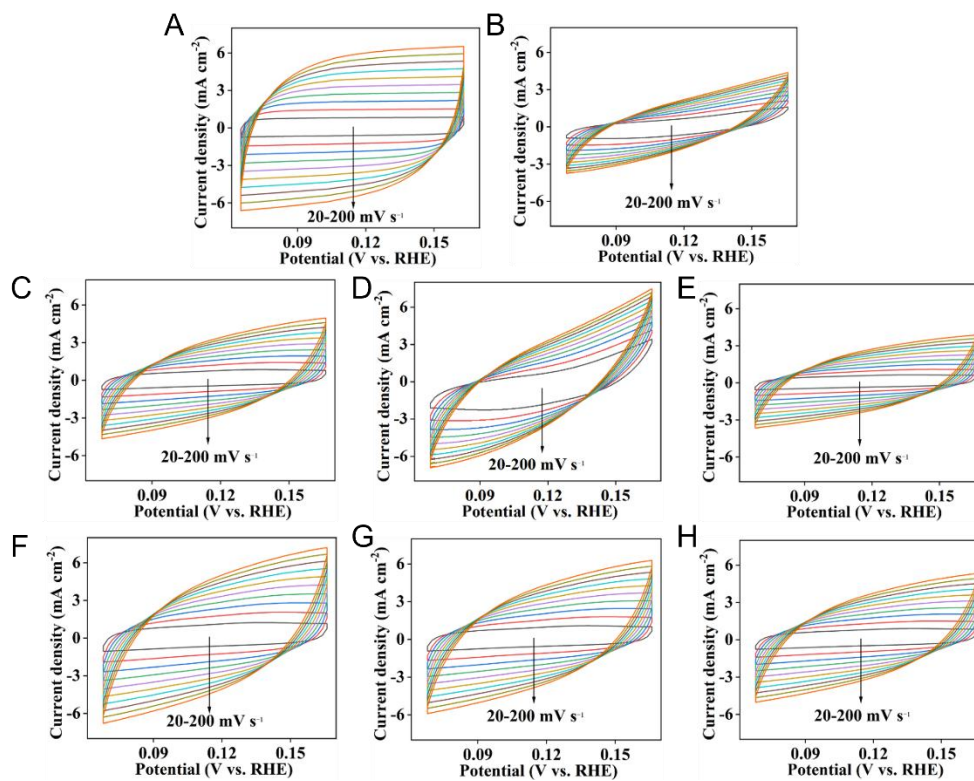
**Supplementary Figure 9.** Cyclic voltammograms of different electrodes in 0.5 M H<sub>2</sub>SO<sub>4</sub>. (A-H) The Cyclic voltammograms of 2D P,N,S-Mo<sub>2</sub>C, 2D Mo<sub>2</sub>C, 2D P-Mo<sub>2</sub>C, 2D N-Mo<sub>2</sub>C, 2D S-Mo<sub>2</sub>C, 2D P,N-Mo<sub>2</sub>C, 2D P,S-Mo<sub>2</sub>C, 2D N,S-Mo<sub>2</sub>C, respectively.



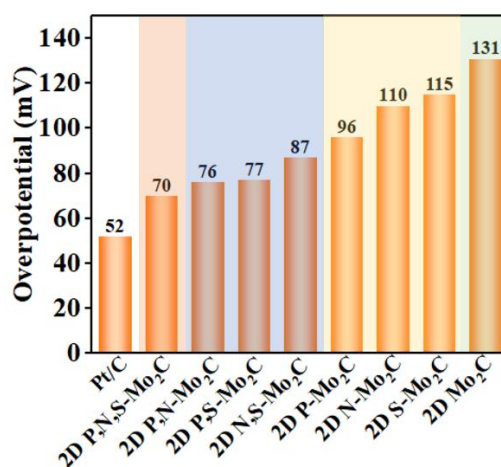
Supplementary Figure 10. Nyquist plots of different samples.



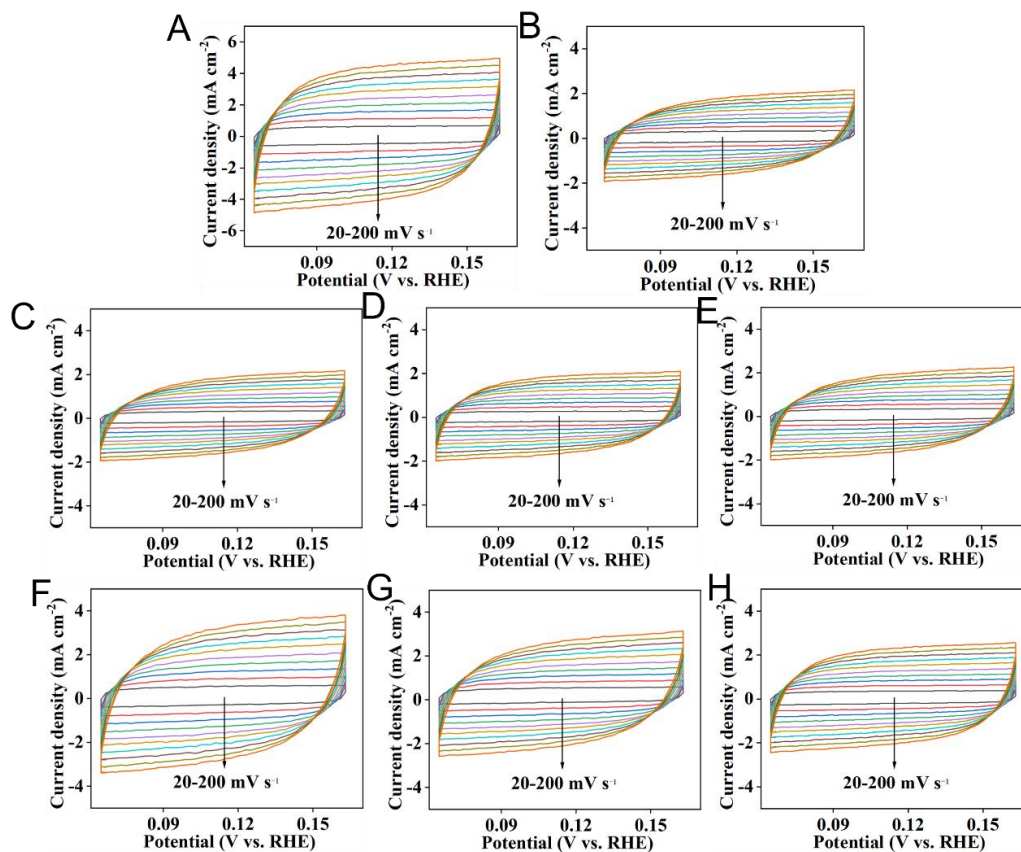
Supplementary Figure 11.  $C_{dl}$  after long-term stability test in 0.5 M  $H_2SO_4$ .



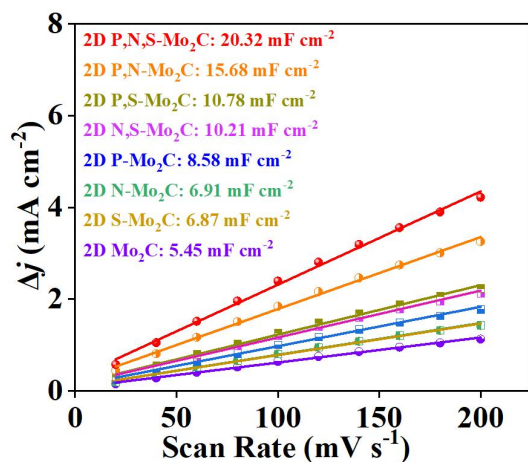
**Supplementary Figure 12.** Cyclic voltammograms of different electrodes in 0.5 M  $\text{H}_2\text{SO}_4$ . (A-H) The cyclic voltammograms of 2D P,N,S-Mo<sub>2</sub>C, 2D Mo<sub>2</sub>C, 2D P- Mo<sub>2</sub>C, 2D N- Mo<sub>2</sub>C, 2D S- Mo<sub>2</sub>C, 2D P,N- Mo<sub>2</sub>C, 2D P,S- Mo<sub>2</sub>C, 2D N,S- Mo<sub>2</sub>C, respectively.



**Supplementary Figure 13.** Overpotentials at 10 mA·cm<sup>-2</sup>.

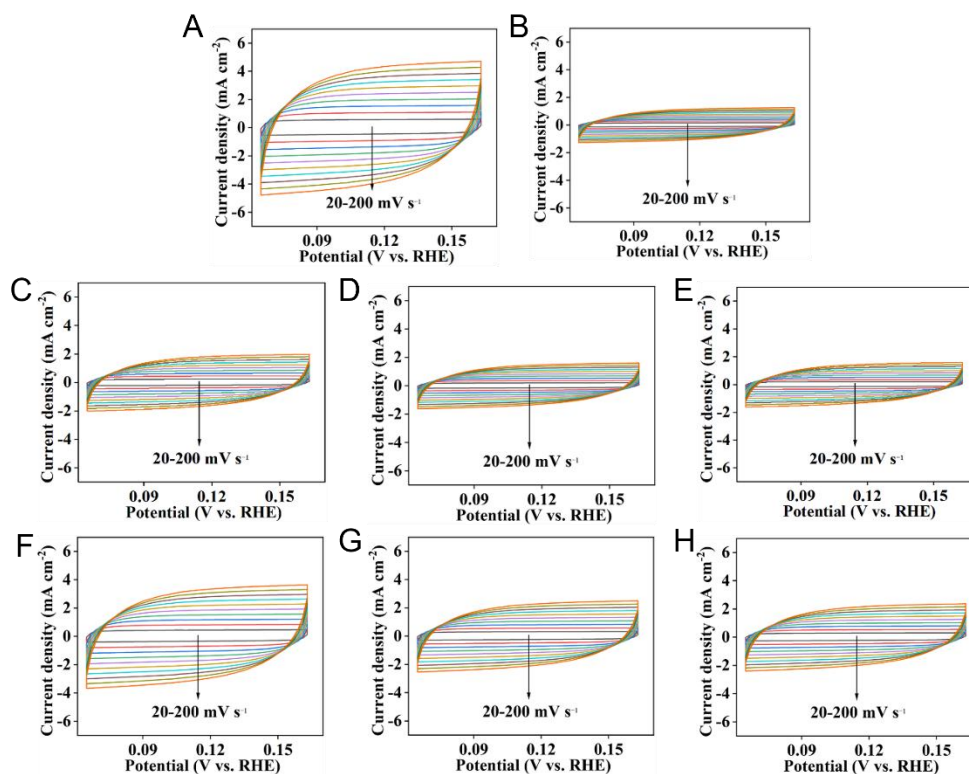


**Supplementary Figure 14.** Cyclic voltammograms of different electrodes in 1 M KOH. (A-H) The Cyclic voltammograms of 2D P,N,S-Mo<sub>2</sub>C, 2D Mo<sub>2</sub>C, 2D P-Mo<sub>2</sub>C, 2D N-Mo<sub>2</sub>C, 2D S-Mo<sub>2</sub>C, 2D P,N-Mo<sub>2</sub>C, 2D P,S-Mo<sub>2</sub>C, 2D N,S-Mo<sub>2</sub>C, respectively.

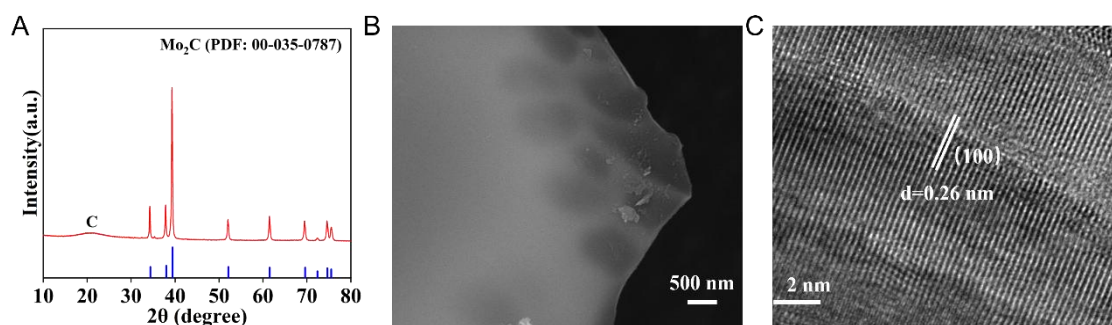


**Supplementary Figure 15.**  $C_{dl}$  after long-term stability test in 1 M KOH.





**Supplementary Figure 16.** Cyclic voltammograms of different electrodes in 1 M KOH. (A-H) The cyclic voltammograms of 2D P,N,S- Mo<sub>2</sub>C, 2D Mo<sub>2</sub>C, 2D P- Mo<sub>2</sub>C, 2D N- Mo<sub>2</sub>C, 2D S- Mo<sub>2</sub>C, 2D P,N- Mo<sub>2</sub>C, 2D P,S- Mo<sub>2</sub>C, 2D N,S- Mo<sub>2</sub>C, respectively.



**Supplementary Figure 17.** (A) The XRD spectrum of 2D P,N,S-Mo<sub>2</sub>C after accelerated durability tests. (B) SEM image of 2D P,N,S-Mo<sub>2</sub>C after accelerated durability tests. (C) TEM image of 2D P,N,S-Mo<sub>2</sub>C after accelerated durability tests.

**Supplementary Tables 1-3**

**Supplementary Table 1.** Parameters of the 2D P,N,S-Mo<sub>2</sub>C from Rietveld refinement. The space group, lattice constants and fitting index of the corresponding from Rietveld refinement.

			<b>2D P,N,S-Mo<sub>2</sub>C</b>
Space group			P63/mmc
Lattice (Å)	Parameters	a	3.015030
		b	3.015030
		c	4.747621
		$\alpha(^{\circ})$	90.000
		$\beta(^{\circ})$	90.000
		$\gamma(^{\circ})$	120.000
		V (Å <sup>3</sup> )	37.376

**Supplementary Table 2.** Comparison of HER properties of different catalysts in 0.5 M H<sub>2</sub>SO<sub>4</sub>

Authors	Material	Electrolyte	Overpotential (mV vs. RHE)	Tafel slop (mV·dec <sup>-1</sup> )
This work	2D N,P,S-Mo <sub>2</sub> C	0.5 M H <sub>2</sub> SO <sub>4</sub>	58	48
Wang <i>et al.</i> <sup>[1]</sup>	Mo <sub>2</sub> C&MoS <sub>2</sub> @N SC <sub>3</sub>	0.5 M H <sub>2</sub> SO <sub>4</sub>	209	85.5
Zhang <i>et al.</i> <sup>[2]</sup>	Co-Mo <sub>2</sub> C-CN <sub>x</sub> -2	0.5 M H <sub>2</sub> SO <sub>4</sub>	116	105
Li <i>et al.</i> <sup>[3]</sup>	PC@Ni-Mo <sub>2</sub> C	0.5 M H <sub>2</sub> SO <sub>4</sub>	156	65
Wang <i>et al.</i> <sup>[4]</sup>	NP-Mo <sub>2</sub> C	0.5 M H <sub>2</sub> SO <sub>4</sub>	210	64
Li <i>et al.</i> <sup>[5]</sup>	Zn, N co-doped Mo <sub>2</sub> C	0.5 M H <sub>2</sub> SO <sub>4</sub>	169.5	62.2
Chi <i>et al.</i> <sup>[6]</sup>	Rich N-doped Mo <sub>2</sub> C	0.5 M H <sub>2</sub> SO <sub>4</sub>	150	61
Shi <i>et al.</i> <sup>[7]</sup>	P-Mo <sub>2</sub> C@C-2.9	0.5 M H <sub>2</sub> SO <sub>4</sub>	89	42
Lu <i>et al.</i> <sup>[8]</sup>	Mo <sub>2</sub> C@2D-NPC	0.5 M H <sub>2</sub> SO <sub>4</sub>	86	62

**Supplementary Table 3.** Comparison of HER properties of different catalysts in 1 M KOH.

Authors	Material	Electrolyte	Overpotential (mV vs. RHE)	Tafel slop (mV·dec <sup>-1</sup> )
This work	2D N,P,S-Mo <sub>2</sub> C	1 K KOH	70	54
Ouyang et al. <sup>[9]</sup>	Mo <sub>2</sub> C@N-CNTs	1 K KOH	170	92
Yang et al. <sup>[10]</sup>	3D Mo <sub>2</sub> C (1:1)	1 K KOH	110	73.9
Lu et al. <sup>[11]</sup>	MoC-Mo <sub>2</sub> C/PNC Ds	1 K KOH	121	60
Jing et al. <sup>[12]</sup>	N-Mo <sub>2</sub> C@NC-1- 120-700	1 K KOH	136	58
Wang et al. <sup>[13]</sup>	NSMB-1.25	1 K KOH	118	74
Yuan et al. <sup>[14]</sup>	Ni/Mo <sub>2</sub> C/NC-60	1 K KOH	180	63
Gong et al. <sup>[15]</sup>	MS-Mo <sub>2</sub> C@NCN S	1 K KOH	98	99
Luo et al. <sup>[16]</sup>	Co <sub>9</sub> S <sub>8</sub> -NSC@Mo <sub>2</sub> C	1 K KOH	89	86.7

**REFERENCES**

1. Wang Q, Yu R, Shen D, et al. One-pot synthesis of Mo<sub>2</sub>C&MoS<sub>2</sub> loaded on N/S co-doped carbon materials as the electrocatalysts for hydrogen evolution reaction. *Fuel* 2022;318:123615. DOI
2. Zhang P, Liu Y, Liang T, et al. Nitrogen-doped carbon wrapped Co-Mo<sub>2</sub>C dual Mott-Schottky nanosheets with large porosity for efficient water electrolysis. *Appl Catal B Environ* 2021;284:119738. DOI
3. Li Z, Fang W, Wu Y, et al. Efficient electrocatalyst for hydrogen evolution reaction: Ni-doped Mo<sub>2</sub>C nanoparticles embedded in porous carbon. *Mater Lett* 2020;280:128611. DOI
4. Wang D, Liu T, Wang J, et al. N, P (S) Co-doped Mo<sub>2</sub>C/C hybrid electrocatalysts for improved hydrogen generation. *Carbon* 2018;139:845-852. DOI

5. Li P, Zheng D, Gao M, et al. Bimetallic MOF-templated fabrication of porous Zn, N Co-doped Mo<sub>2</sub>C for an efficient hydrogen evolution reaction. *ACS Appl Energy Mater* 2021;4:8875-82. [DOI](#)
6. Chi J Q, Yan K L, Gao W K, et al. Solvothermal access to rich nitrogen-doped molybdenum carbide nanowires as efficient electrocatalyst for hydrogen evolution reaction. *J Alloy Compd* 2017;714:26-34. [DOI](#)
7. Shi Z, Nie K, Shao Z J, et al. Phosphorus-Mo<sub>2</sub>C@carbon nanowires toward efficient electrochemical hydrogen evolution: composition, structural and electronic regulation. *Energy Environ Sci* 2017;10:1262-71. [DOI](#)
8. Lu C, Tranca D, Zhang J, et al. Molybdenum carbide-embedded nitrogen-doped porous carbon nanosheets as electrocatalysts for water splitting in alkaline media. *ACS Nano* 2017;11:3933-42. [DOI](#)
9. Ouyang T, Ye Y Q, Wu C Y, et al. Heterostructures Composed of N-Doped Carbon Nanotubes Encapsulating Cobalt and β-Mo<sub>2</sub>C Nanoparticles as Bifunctional Electrodes for Water Splitting. *Angew Chem Int Ed* 2019;58:4923-28. [DOI](#)
10. Yang X, Cheng J, Yang X, et al. Facet-tunable coral-like Mo<sub>2</sub>C catalyst for electrocatalytic hydrogen evolution reaction. *Chem Eng J* 2023;451:138977. [DOI](#)
11. Lu X F, Yu L, Zhang J, et al. Ultrafine dual-phased carbide nanocrystals confined in porous nitrogen-doped carbon dodecahedrons for efficient hydrogen Evolution reaction. *Adv Mater* 2019;31:e1900699. [DOI](#)
12. Jing Q, Zhu J, Wei X, et al. An acid-base molecular assembly strategy toward N-doped Mo<sub>2</sub>C@C nanowires with mesoporous Mo<sub>2</sub>C cores and ultrathin carbon shells for efficient hydrogen evolution. *J Colloid Interf Sci* 2021;602:520-533. [DOI](#)
13. Wang, X., Xia L, Guo C, et al. Interfacial engineering of N, S-doped Mo<sub>2</sub>C-Mo/C heterogeneous nanorods for enhanced alkaline hydrogen evolution. *Appl Surf Sci* 2023;614:156276. [DOI](#)
14. Yuan Q, Chen W, Hu R, et al. Metal-polydopamine derived N-doped carbon nanorod wrapping Ni and Mo<sub>2</sub>C nanoparticles for efficient hydrogen evolution reaction. *Mater Lett* 2022;307:130989. [DOI](#)
15. Gong T, Liu Y, Cui K, et al. Binary molten salt in situ synthesis of sandwich-structure hybrids of hollow β-Mo<sub>2</sub>C nanotubes and N-doped carbon nanosheets for hydrogen evolution reaction. *Carbon Energy* 2023;e349. [DOI](#)
16. Luo X, Zhou Q, Du S, et al. Porous Co<sub>9</sub>S<sub>8</sub>/Nitrogen, Sulfur-Doped Carbon@Mo<sub>2</sub>C Dual Catalyst for Efficient Water Splitting. *ACS Appl Mater Inter* 2018;10:22291-302. [DOI](#)